



Pelagia Research
Library

Pelagia Research Library

Der Chemica Sinica, 2016, 7(3):16-25



Pelagia Research
Library
ISSN: 0976-8505
CODEN (USA) CSHIA5

Chemical, electrochemical and quantum evaluation of L-Methione (LM) as corrosion inhibitor for mild steel in HCl solution

Ekerete Jackson^{1*}, K. E. Essien² and I. B. Obot¹

¹Department of Chemistry, Faculty of Science, University of Uyo, P.M.B 1017, Uyo, AkwaIbom, State, Nigeria

²Department of Science Technology, AkwaIbom State Polytechnic, Ikot Osurua, P. M. B. 1200, AkwaIbom State, Nigeria

ABSTRACT

Chemical, electrochemical and quantum chemical techniques were used to study the corrosion inhibition and adsorption processes of L-Methione (LM). The results obtained indicate that the inhibition efficiency increases with decreasing temperature and increasing concentration of inhibitor. It has been shown that the adsorption of LM on mild steel obeys the Temkin adsorption isotherm at all studied temperatures with negative values of ΔG_{ads} suggesting a stable and a spontaneous inhibition process. Polarization data show that the compound behaves as a mixed type inhibitor. Polarization parameters were determined with maximum value of inhibition efficiency for 5×10^{-4} M concentration of the inhibitor at 303 K is 79.9 %. From Nyquist plot of electrochemical impedance spectroscopy, polarization resistance (R_p) increased with increasing inhibitor concentration whereas double layer capacitance (C_{dl}) decreased indicating a decrease in local dielectric constant suggesting that the inhibitors function by forming a protective layer at the metal surface. Quantum chemical approach was further used to calculate some electronic properties of the molecule in order to ascertain any correlation between the inhibitive effect and molecular structure of LM.

Key words: L-Methione (LM), electrochemical impedance spectroscopy, corrosion inhibition, Temkin adsorption isotherm, mild steel (MS).

INTRODUCTION

Metal surfaces are extensively used in a variety of industrial applications such as petroleum, textile and marine industries as a component of pumps or valves that carry various types of substances. However some of these substances are highly corrosive and include such solutions as hydrochloric acid [1]. For instance, in the petroleum industry hydrochloric acid solutions are widely utilized for oil well acidizing, while in marine industries hydrochloric acid is largely used for pickling purposes [2]. The corrosion of metal surfaces causes huge financial damages to the industries annually, what has lead to an increase in the search for substances that can slow down or prevent corrosion rate. Corrosion is a major concern globally due to the destructive attack of metals by chemical and electrochemical reactions. Though corrosion action seems slow and negligible, it is complex to analyze because it involves a large number of variables. Corrosion is defined as the process in which a metal or its alloy is consistently transformed from the pure metallic form to the oxidized state by interacting with the environment [1,2].

Corrosion can take place in different media: acidic, alkaline or neutral; and in various ways either over the entire surface of the metal, electrochemically between the different metals or between two points on the metal surface that have different chemical activity. Corrosion consists of at least two reactions on the surface of the corroding metal; one is the oxidation, also referred to as anodic half reaction; the other is reduction reaction, also referred to as cathodic half reaction [3].

Negligence of the basic corrosion protection technology can lead to expensive problems not only financial but also with respect to safety as well. This is why anti-corrosion techniques are of much importance and they can be determined at two levels: prevention at the stage of design, the “cure” stage after corrosion has set in. These include engineering design, anodic protection, lining, cathodic protection and corrosion inhibition. Corrosion control of metals is of technical, economic, environmental, and aesthetical importance. The use of inhibitors is one of the best options of protecting metals and alloys against corrosion [4].

L – Methionine(LM) has not been investigated as corrosion inhibitor. Hence, this work deals with the study of the corrosion inhibition properties of this compound. The aim of this study was to determine the inhibition efficiency of LM as an inhibitor for the corrosion of mild steel in 2 M HCl. Three techniques were employed to carry out the measurements: (a) chemical (weight loss) (b) electrochemical (potentiodynamic polarization) and (c) molecular modeling.

The molecular structure of L – Methionine(LM) is as shown below:

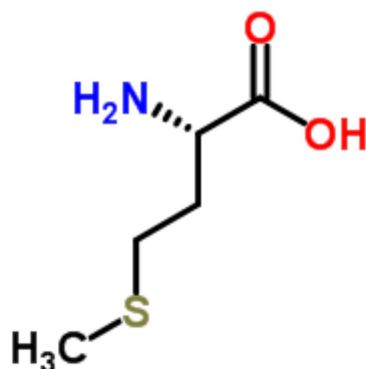


Figure 1: The chemical structure of L – Methionine(LM)

MATERIALS AND METHODS

2.1 Materials

Material used for the study was mild steel sheet. The sheet was mechanically pressed cut into coupons of dimensions 5 x 4 x 0.11 cm for weight loss studies and 2 x 1.5 x 0.11 cm for electrochemical studies with a hole made for insertion of the hooks. The coupons were polished with series of emery paper of variable grades starting with the coarsest and then proceeding in steps to the finest (600) grade, degreased with ethanol, dipped in acetone and allowed to dry in the air before it was preserved in a desiccator [5, 6,7,8,9]. All reagents used for the study were Analar grade and distilled water was used for their preparation. The chemical composition of the mild steel used is as shown in Table 1.

Table 1. Chemical Composition of Mild Steel Samples (Wt %)

| | |
|----|--------|
| C | 0.17 |
| Si | 0.26 |
| Mn | 0.46 |
| P | 0.0047 |
| S | 0.017 |
| Fe | Bal. |

2.2 Gravimetric measurements

The apparatus and procedure followed for the weight loss measurements were as previously reported [10-16]. The corrodent concentration was kept at 2 M HCl and the volume of the test solution used was 100 mL. All tests were made in aerated solutions. The difference between the weight at a given time and the initial weight of the coupons was taken as the weight loss which was used to compute the corrosion rate given by [11]:

$$\text{Corrosion rate, } \rho = \frac{\Delta W}{At} \quad (1)$$

Where, ΔW is the weight loss, A is the total area of the mild steel coupon, t is the corrosion time and ρ is the corrosion rate.

$$\text{Surface Coverage, } \theta = \frac{\rho_1 - \rho_2}{\rho_1} \quad (2)$$

$$\text{Inhibition efficiency, \% I} = \frac{\rho_1 - \rho_2}{\rho_1} \times 100 \quad (3)$$

Where, ρ_1 and ρ_2 are the corrosion rates of the mild steel in 2 M HCl (blank) in the absence and presence of inhibitor respectively.

2.3 Polarization measurement

The working electrode was immersed in test solution for 30 minutes until a steady state open circuit potential (E_{ocp}) was obtained. The polarization curve was recorded under potentiodynamic polarization conditions and under air atmosphere and it was controlled by a personal computer. After the open circuit potential had been established, dynamic polarization curves were obtained at a scan rate of 1 mV/s in the potential range from - 0.25 V to 0.25 V. Corrosion current density (i_{corr}) values were obtained by the Tafel extrapolation method. All potentials were measured against SCE. The percentage inhibition efficiency (η), was calculated using the equation [17]

$$\eta(\%) = \frac{i_{corr}^o - i_{corr}}{i_{corr}^o} \times 100 \quad (4)$$

Where, i_{corr}^o and i_{corr} are values of corrosion current density in the absence and presence of inhibitor respectively.

2.4 Electrochemical impedance spectroscopy measurement

The electrochemical impedance spectroscopy measurements were carried out over a frequency domain from 10 Hz to 100,000 Hz at 303 K using amplitude of 5 mV RMS peak to peak with an ac signal at the open circuit potential and an air atmosphere. The impedance data were obtained using Nyquist plots and the polarization resistance R_p was obtained from the diameter of the semicircle in Nyquist plot. The polarization resistance (R_p) includes charge transfer resistance (R_{ct}), diffuse layer resistance (R_d), the resistance of accumulated species at the metal/solution interface (R_a) and the resistance of the film (in the presence of the inhibitor) at the metal surface (R_f). The percentage inhibition efficiency (η) was calculated from the polarization resistance values obtained from the impedance measurements according to the relation [17]

$$\eta(\%) = \frac{R_p(inh) - R_p}{R_p(inh)} \times 100 \quad (5)$$

Where $R_{p(inh)}$ and R_p are the charge transfer resistance in the presence and absence of inhibitor respectively. The double layer capacitance (C_{dl}) was calculated using the equation

$$C_{dl} = \frac{1}{2\pi f_{max} R_p} \quad (6)$$

Where f_{max} is the frequency at the maximum in the Nyquist plot.

2.5 Computational details

First principle calculations were carried out using density functional theory (DFT) under the generalized gradient approximation (GGA) with Perdew – Burke - Eruzerhof (PBF) exchange correlation functional as implemented in Dmol³ module using material studio software package version 6.0. The quantum chemical indices considered were: the energy of the highest occupied molecular orbital (E_{HOMO}), the energy of the lowest unoccupied molecular orbital (E_{LUMO}), Energy gap = $E_{HOMO} - E_{LUMO}$, total energy, and Mulliken charges [18, 19].

RESULTS AND DISCUSSION

3.1 Gravimetric study

The weight loss (gravimetric measurements) for the mild steel in 2 M HCl containing different concentrations of LM as function of time at 323 K is presented in Figure 2.

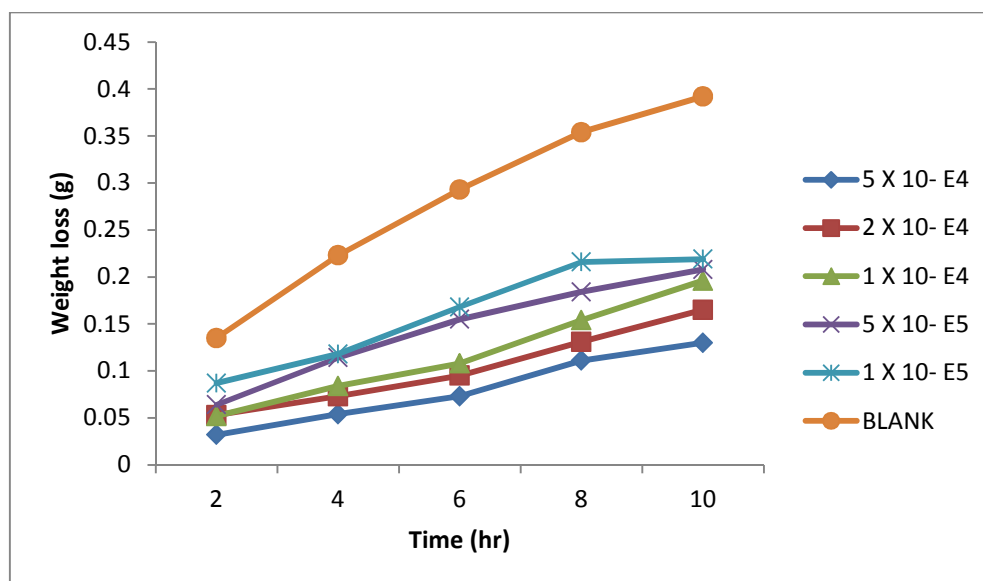


Figure 2. Variation of weight loss with time for the corrosion of mild steel in 2 M HCl containing various concentrations of concentrations of LM at 323 K

The corrosion inhibition efficiency (% IE), corrosion rate (CR) and surface coverage (Θ) of LM after 10 hours of immersion at different temperatures (303 to 333K) are presented in Table 1. It is observed that the inhibition efficiency increased with increasing concentration of the inhibitor. In the absence of any inhibitor, the corrosion rate of mild steel increased steeply with increase in temperature. The corrosion rate was much lower in the presence of inhibitors than in the absence of any inhibitor at any temperature resulting in the retardation of the rate at which the metal goes into solution. The plot of weight loss versus time at 323 K for the blank and various concentrations of the inhibitor is shown in figure 2. For the blank (2 M HCl) the graph is uppermost due to the high corrosion rate; and the lower graphs are for various concentrations of the inhibitor indicating inhibition (reduction in corrosion rate) with increasing inhibitor concentrations.

TABLE 2: Calculated values of corrosion rate of mild steel (CR), degree of surface coverage (Θ) and inhibition efficiency (% IE) of LM at 303 to 333K

| Inhibitor | Conc. $\times 10^{-4}$ (M) | 303 K | | | 313 K | | | 323 K | | | 333 K | | |
|-----------|-------------------------------|--|----------|------|--|----------|------|--|----------|------|--|----------|------|
| | | CR $\text{gcm}^{-2}\text{m}^{-1}$ $\times 10^{-4}$ | Θ | % IE |
| | Blank | 8.55 | - | - | 12.75 | - | - | 19.60 | - | - | 29.60 | - | - |
| LM | 5.0 | 3.90 | 0.54 | 54 | 5.10 | 0.60 | 60 | 6.50 | 0.67 | 67 | 5.95 | 0.80 | 80 |
| | 2.0 | 4.40 | 0.49 | 49 | 6.12 | 0.52 | 52 | 8.25 | 0.58 | 58 | 8.60 | 0.71 | 71 |
| | 1.0 | 4.90 | 0.43 | 43 | 6.75 | 0.47 | 47 | 9.80 | 0.50 | 50 | 11.00 | 0.63 | 63 |
| | 0.5 | 5.13 | 0.40 | 40 | 7.14 | 0.44 | 44 | 10.38 | 0.47 | 47 | 13.05 | 0.56 | 56 |
| | 0.1 | 5.55 | 0.35 | 35 | 7.77 | 0.39 | 39 | 10.97 | 0.44 | 44 | 15.10 | 0.49 | 49 |

The adsorption characteristics of the inhibitor (LM) were investigated by fitting data obtained for the degree of surface coverage in different adsorption isotherms including Langmuir, Temkin, Freundlich, Florry-Huggins, Frumkin and Bockris-Swinkel adsorption isotherms. The test indicated that the adsorption was best described by Temkin adsorption model which is expressed as

$$\exp(f\theta) = K_{\text{ads}} C \quad (4)$$

K_{ads} is the equilibrium constant of the adsorption process, C is the inhibitor concentration, Θ is the surface coverage, and f is the factor of energetic inhomogeneity. Figure 3 is a plot of surface coverage against logarithm of inhibitor concentration. The correlation coefficient (R^2) was in the range 0.937 to 0.997 for the inhibitor which is close to unity, indicating that the adsorption of the inhibitors is consistent with Temkin adsorption model.

The parameter f is defined as

$$f = -2a \quad (5)$$

Where, a is molecular interaction parameter. The calculated values of ' a ' and equilibrium constant of the adsorption process (K_{ads}) obtained from Temkin adsorption plots are shown in table 5.

Table 3. Temkin parameters for the adsorption of LM on mild steel surface at 303 - 333 K

| Inhibitor | T (K) | Intercept | Slope | K (mol/L) | f | a | $-\Delta G$ (kJ/mol) | R^2 |
|-----------|-------|-----------|-------|-----------|--------|---------|-------------------------|-------|
| LM | 303 | 0.301 | 0.047 | 604.4 | 21.777 | -10.639 | 26.25 | 0.992 |
| | 313 | 0.334 | 0.050 | 796.3 | 20.000 | -10.000 | 27.84 | 0.972 |
| | 323 | 0.361 | 0.057 | 563.0 | 17.544 | -8.772 | 27.80 | 0.937 |
| | 333 | 0.407 | 0.077 | 197.5 | 12.987 | -6.494 | 25.75 | 0.997 |

$$\exp(-2a\theta) = K_{\text{ads}} C \quad (6)$$

The sign between f and a is reverse; that is, if $a < 0$, then $f > 0$ and if $a > 0$, then $f < 0$. Accordingly, if $f < 0$, mutual repulsion of molecules occurs and if $f > 0$, attraction occurs [20, 21]. From Table 3, the values of $f > 0$ indicating that attraction exist in the adsorption layer.

K_{ads} denotes the strength between adsorbate and adsorbent. Large values of K_{ads} indicate more efficient adsorption and better inhibition efficiency. From table 3, values of K_{ads} are large which indicate strong interaction between inhibitor and mild steel surface.

$$K_{\text{ads}} = \frac{1}{55.5} \exp\left(\frac{\Delta G_{\text{ads}}^{\circ}}{RT}\right) \quad (7)$$

Where R is the molar gas constant, T is temperature and 55.5 is concentration of water in solution expressed in molar.

$$\log K_{\text{ads}} = 1.744 - \frac{\Delta G_{\text{ads}}^{\circ}}{2.303RT} \quad (8)$$

The standard free energy of adsorption ($\Delta G_{\text{ads}}^{\circ}$) was calculated from the above equation and presented in table 3. The negative values of the $\Delta G_{\text{ads}}^{\circ}$ reflect the spontaneity of the adsorption process and stability of the adsorped layer on the mild steel.

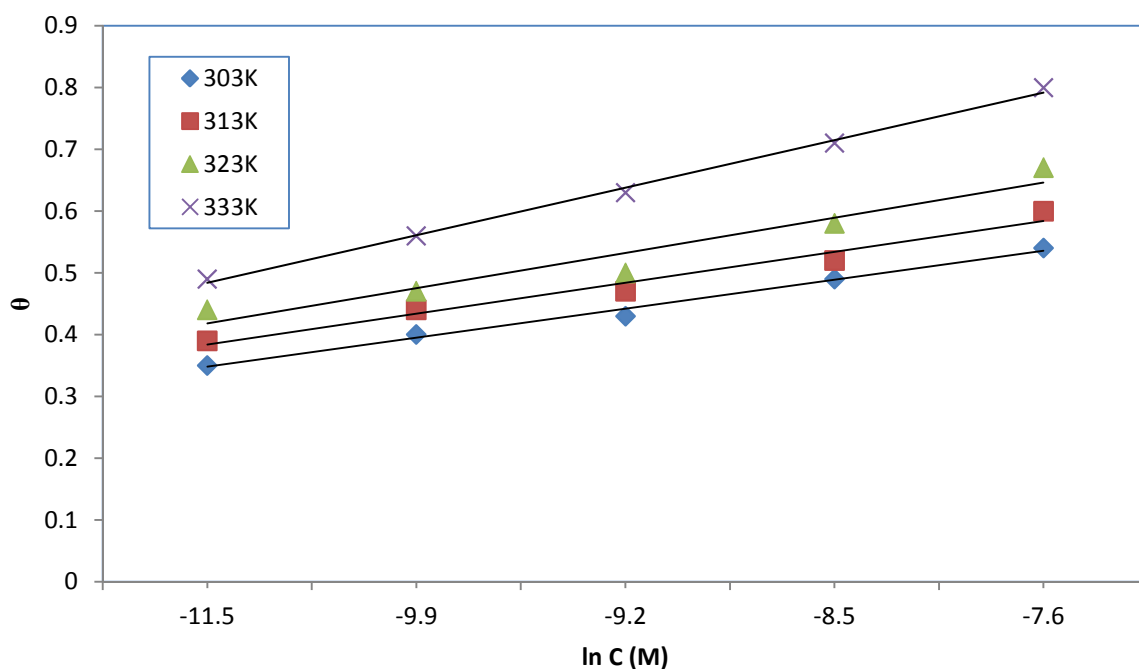


Figure 3: Temkin isotherm for the adsorption of LM on mild steel surface

3.2 Electrochemical Impedance Study (EIS).

The electrochemical impedance data are depicted as Nyquist plot in Figure 4. Analysis of the Nyquist plot (figure 4) showed a depressed capacitance loop which arises from the time constant of the electrical double layer and charge transfer resistance. The deviation of semicircles from perfect circular shape is often referred to the frequency dispersion of interfacial impedance [22]. This behavior is usually attributed to the inhomogeneity of the metal surface arising from surface roughness or interfacial phenomena [23], which is typical for solid metal electrodes [24]. The polarization resistance R_p was obtained from the diameter of the semicircle in Nyquist plot. The polarization resistance (R_p) includes charge transfer resistance (R_{ct}), diffuse layer resistance (R_d), the resistance of accumulated species at the metal/solution interface (R_a) and the resistance of the film (in the presence of the inhibitor) at the metal surface (R_f). From the values of polarization resistance (R_p) and double layer capacitance (C_{dl}) obtained from Nyquist plots and the calculated inhibition efficiency value (η %), it is obvious that the value of R_p increased with increasing concentration of inhibitor. The increase in R_p values is attributed to the formation of an insulating protective film at the metal/solution interface. It is also obvious that the value of C_{dl} decreased upon the addition of each of the inhibitors, indicating a decrease in the local dielectric constant and/or an increase in the thickness of the electric double layer suggesting that the inhibitors functioned by forming a protective layer at the metal surface. Generally, when a non-ideal frequency response is present, it is commonly accepted to employ the distributed circuit elements in the equivalent circuits. What most widely used is the constant phase element (CPE), which has a non-integer power dependence on the frequency [25, 26]. Thus, the equivalent circuit depicted in Figure 6 is employed to analyze the impedance spectra, where R_s represents the solution resistance, R_t denotes the charge-transfer resistance, and a CPE instead of a pure capacitor represents the interfacial capacitance.

As seen from Table 4, the C_{dl} values decrease with the increase of LM concentration, which suggests that LM functions by adsorption on the mild steel surface. It is inferred that the LM molecules gradually replace the water molecules by adsorption at the metal/solution interface, which leads to the formation of a protective film on the mild steel surface and thus decreases the extent of the dissolution reaction [27]. Moreover, the increase of LM concentration leads to the increase of R_{ct} and η % values.

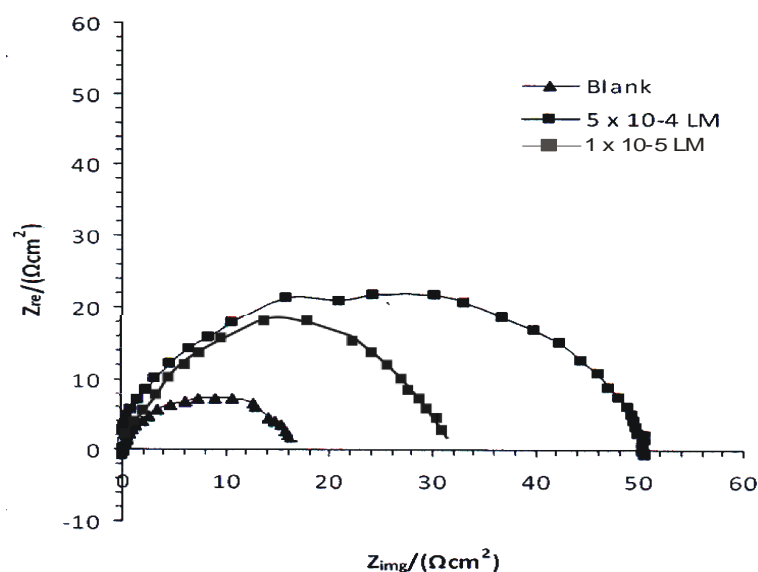


Figure 4: Nyquist plot for the corrosion of mild steel in 2 M HCl solution in the absence and presence of L – METHIONE (LM) at 30°C

TABLE 4: Electrochemical impedance spectroscopy parameters and inhibition efficiency (η %) for mild steel in 2M HCl solution in the presence and absence of LM at 303 K

| Inhibitor | Concentration M X 10 ⁻⁴ | R _p (R _{ct}) Ω cm ² | f _{max} | C _{dl} | η% |
|-----------|---------------------------------------|--|------------------|-----------------|------|
| BLANK | | 16.89 | 7.55 | 1248 | |
| LM | 0.1 | 27.8 | 13.69 | 530 | 31.2 |
| | 1 | 50 | 21.84 | 160 | 56.9 |

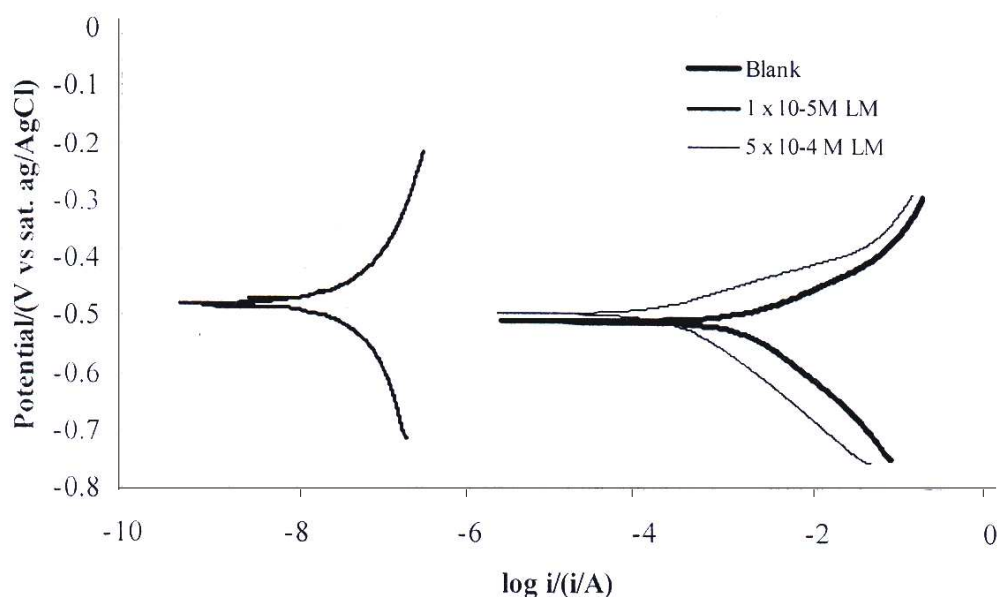


Figure 5: Potentiodynamic polarization curve for mild steel in 2 M HCl in the presence and absence of L – METHIONE (LM) at 30°C

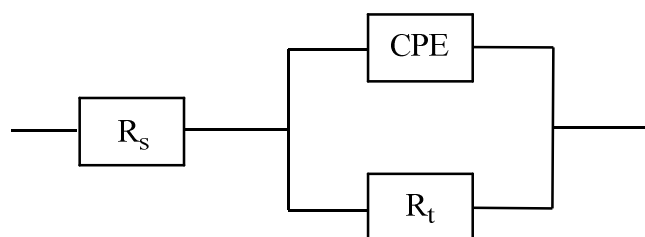


Fig. 6. Equivalent circuit for MS in 2 M HCl solution.

TABLE 5: Electrochemical parameters and inhibition efficiency ($\eta\%$) obtained from polarization studies of mild steel in 2M HCl solution in the presence and absence of LM at 303 K

| Inhibitor | Concentration $M \times 10^{-4}$ | E_{corr} Vm | i_{corr} $\mu A \text{ cm}^{-2}$ | β_c $m \text{ V dec}^{-1}$ | β_a $\mu A \text{ m V dec}^{-1}$ | $\eta\%$ |
|-----------|-------------------------------------|------------------|---------------------------------------|-------------------------------------|---|----------|
| BLANK | | 510 | 1563 | 157 | 103 | |
| LM | 0.1 | -479 | 390 | 273 | 212 | 70.3 |
| | 1.0 | -496 | 234 | 116 | 60 | 79.9 |

3.3 Potentiodynamic polarization measurements

The anodic and cathodic potentiodynamic curves for mild steel in 2M HCl solutions in the absence and presence of 1×10^{-5} M and 5×10^{-4} M of the LM at 30°C is shown in Figure 5. The nature of the polarization curves remained the same in the absence and presence of the inhibitor, but the curves shifted towards lower current density in the presence of the inhibitor suggesting that the inhibitor molecules retard the corrosion process without changing the mechanism of the corrosion process. The polarization curves exhibit cathodic and anodic polarization curves with well defined Tafel regions. The electrochemical parameters namely: corrosion potential (E_{corr}), corrosion current densities (i_{corr}), anodic Tafel slope (β_a), cathodic Tafel slope (β_b) and percentage inhibition efficiency ($\eta\%$) determined from the polarization curves are summarized in Table 5 with a maximum value for 5×10^{-4} M concentration of the inhibitors at 303 K as 79.9%.

As observed, the corrosion potential (E_{corr}) has no definite shift and the corrosion current densities (i_{corr}) decreases when the concentrations of the inhibitors increase indicating that the inhibitors adsorbed on the metal surface, and hence the inhibition efficiency increased with increasing inhibitor concentration causing small change in E_{corr} values

implying that the inhibitors act as mixed type inhibitors affecting both the anodic and cathodic reactions. If the displacement in E_{corr} is more than ± 85 mV/SCE with respect to the corrosion potential of the blank, the inhibitor can be considered as cathodic or anodic type. If the change in E_{corr} is less than 85mV/SCE, the corrosion inhibitor can be regarded as mixed type [28, 29]. Maximum displacement is 31 mV/SCE which indicates that the inhibitor is mixed type.

3.4 Theoretical calculations

The optimized geometry of LM is shown in Figure 7 and their corresponding frontier molecular orbitals (HOMO and LUMO) are shown in Figures 8 and 9. The energy levels viz: E_{HOMO} , E_{LUMO} and ΔE calculated are depicted in Table 6. The energies of the frontier molecular orbital: E_{HOMO} and E_{LUMO} are significant parameters for the prediction of the reactivity of any chemical species. The frontier molecular theory describes that the formation of a transition state is due to an interaction between frontier molecular orbitals (HOMO and LUMO) of reacting species [30]. E_{HOMO} is associated with electron-donating ability of the inhibitor. As such, the inhibition efficiency of inhibitor is expected to increase with increasing value of E_{HOMO} since this indicates increasing ease of donating electrons to the vacant d-orbital of the metal. E_{LUMO} , on the other hand, is associated with the ability of the molecule to accept electron, therefore decreasing values of E_{LUMO} suggest better inhibition efficiency [31]. The energy gap of an inhibitor ($\Delta E = E_{\text{LUMO}} - E_{\text{HOMO}}$) is an important stability index and is used to develop theoretical models for explaining structure and conformation barriers in molecular systems. The smaller the energy gap, the better is the expected inhibition efficiency of the compound [32]. According to the results in Table 4, the highest value of E_{HOMO} -4.494eV and the lowest value of ΔE -1.238eV were found for L – METHIONE (LM) affirming that L – METHIONE (LM) has more potency to be adsorbed on the mild steel. The global hardness is the inverse of the global softness ($\eta = 1/S$). Values of S and η are presented in Table 4. The hard and soft acids and bases principle requires that a reaction between an acid and a base is favored when global softness difference is minimal. Also, a hard molecule has a large energy gap while a soft molecule has a low energy gap.

TABLE 6: Quantum Chemical parameters for L – METHIONE (LM)

| Inhibitor | LM |
|--------------------------------|--------|
| E_{HOMO} (eV) | -4.494 |
| E_{LUMO} (eV) | -1.238 |
| ΔE (eV) | 3.711 |
| Absolute electronegativity(eV) | 3.094 |
| Global hardness (eV) | 1.856 |
| Global softness (eV) | 0.539 |

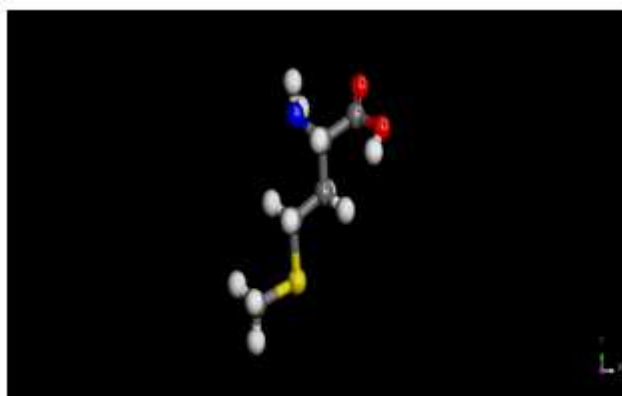


Figure 7. DFT-B3LYP Optimized Structure of L – METHIONE (LM)

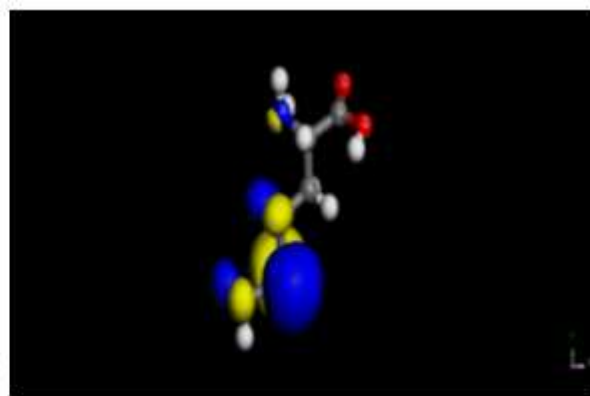


Figure 8. HOMO electronic density of L – METHIONE (LM) molecule

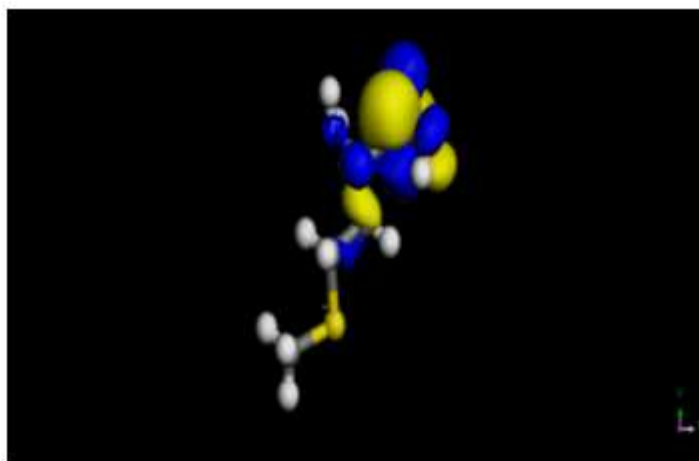


Figure 9. LUMO electronic density of L – METHIONE (LM) molecule

CONCLUSION

1. L – Methione (LM) showed good inhibition efficiency for the corrosion of mild steel in 2M HCl solutions.
2. The corrosion inhibition is due to the adsorption of the inhibitor on the metal surface by physical and chemical adsorption.
3. The potentiodynamic polarization curves showed that the inhibitor is mixed type inhibitor.
4. Computational calculations show that apart from LM molecule adsorbing as cationic species on the mild steel surface, it can also adsorb as molecular species using oxygen, nitrogen and sulphur as its active centres.

REFERENCES

- [1] N. O. Eddy, F. E. Awe, C. E. Gimba, N. O. Ibsi, E. E. Ebenso, *Int. J. Electrochem. Sci.*, 6 (2011) 931.
- [2] G. Schmitt, *Br. Corros. J.* 19 (1984) 165.
- [3] M. G. Fontana, N. D. Green, (1967) Corrosion Engineering. New York, McGraw-Hill Book Company
- [4] A. I. Onuchukwu, (2008) Electrochemical technology. Ibadan. Spectrum books limited.
- [5] I.B. Obot, N.O. Obi-Egbedi, *Surf. Rev. Lett.* 15(6) (2008) 903
- [6] M. Lashkari, M. R. Arshadi, *J. Chem. Phys.* 299 (2004) 131.
- [7] I.B. Obot, N.O. Obi-Egbedi, *Corros. Sci.* 52 (2010) 198.
- [8] N.O. Eddy, E.E. Ebenso, *Int. J. Electrochem. Sci* 5 (2010) 731.
- [9] P.C. Okafor, E.E. Ebenso, U.J. Ekpe, *Int. J. Electrochem. Sci* 5 (2010) 978.
- [10] K. F. Khaled, *Corrosion Science* 50: (2010) 2905 – 2916
- [11] I.B. Obot, N.O. Obi-Egbedi, *Corros. Sci.* 52 (2010) 198.
- [12] N.O. Eddy, E.E. Ebenso, *Int. J. Electrochem. Sci* 5 (2010) 731.
- [13] P.C. Okafor, E.E. Ebenso, U.J. Ekpe, *Int. J. Electrochem. Sci* 5 (2010) 978.
- [14] I.B. Obot, N.O. Obi-Egbedi, S. A. Umoren, E. E. Ebenso, *Int. J. Electrochem. Sci* 5 (2010) 994.
- [15] E.E. Ebenso, H. Alemu, S.A. Umoren, I.B. Obot, *Int. J. Electrochem. Sci.* 3 (2008) 1325.
- [16] N. O. Obi-Egbedi, I. B. Obot, *Arab. J. Chem.* (2010). doi:10.1016/J.arabjc.2010.10.004.
- [17] H. Ashassi-Sorkhabi, B. Shaabani, and D. Seifzadeh, *Applied surf. Sci.* 239(2005)154-164
- [18] A. Popova, E. Sokolova, S. Raicheva, M. Chritov, *Corros. Sci.* 45 (2003) 33 - 41
- [19] G. Quartarone, G. Moretti, A. Tassan, A. Zingale, *Mater. Corros* 45(1994) 641 - 647
- [20] M. Abdallah, E. A. Helal and A. S. Fouda, *Corros. Sci.* 48 (2006) 1639- 1645
- [21] Umoren, S. A., Obot, I. B., Ebenso, E. E. and Okafor, P. C. *Portugaliae Electrochimica Acta* 26 (2008) 267 - 287
- [22] F. Mansfeld, M. W. Kendig, S. Tsai, *Corros. Sci.* 38 (1982) 570 – 580.
- [23] S. Martinez, M. Metikos-Hukovic, *J. Appl. Electrochem.* 33 (2003) 1137 – 1142.
- [24] F. Bentiss, M. Lebrini, H. Vezin, F. Chai, M. Traisnel, M. Laggrenne, *Corros. Sci.* 51 (2009) 2165 – 2173.
- [25] J. L. Trinstancho-Reyes, M. Sanchez-Carrillo, R. Sandoval-Jabalera, V. M. Orozco-Carmona, F. Almeraya-Calderon, J. G. Chacon-Nava, J. G. Gonzalez-Rodriguez, A. Martinez-Villafarie, *Int. J. Electrochem. Sci.* 6 (2011) 419-431.
- [26] M. Kissi, M. Bouklah, B. Hammouti, M. Benkaddour, *Appl. Surf. Sci.* 252 (2006) 4190-4197.
- [27] F. Bentiss, M. Traisnel, M. Laggrenne, *Corros. Sci.* 42 (2000) 127 – 146.

-
- [28] M. Yadav , D. Behera, S. Kumur, , R. R. Sinha, *Industrial and engineering chemistry research* 52 (2013) 6318 - 6328
- [29] M..Yadav, S. Kumar, D. Behera, *Journal of Metallurgy* 1 (2013) 1 - 15
- [30] K. Fukui, Springer-Verlag, New york, **1975**.
- [31] G. Gokhan, *Corros. Sci.* 50 (2008), Pp. 2961 – 2992.
- [32] H. E. El Ashry, A. El Nemr, S. A. Esawy, and S. Ragab, *Electrochim. Acta* 51 (2006), Pp. 3957 – 3968.